Actomyosin bundles serve as a tension sensor and a platform for ERK activation

Hiroaki Hirata[1], Mukund Gupta[1], Sri Ram Krishna Vedula[1,†], Chwee Teck Lim[1,2,3], Benoit Ladoux[1,4] & Masahiro Sokabe[1,5,*]

Abstract

Tensile forces generated by stress fibers drive signal transduction events at focal adhesions. Here, we report that stress fibers per se act as a platform for tension-induced activation of biochemical signals. The MAP kinase, ERK is activated on stress fibers in a myosin II-dependent manner. In myosin II-inhibited cells, uniaxial stretching of cell adhesion substrates restores ERK activation on stress fibers. By quantifying myosin II- or mechanical stretch-mediated tensile forces in individual stress fibers, we show that ERK activation on stress fibers correlates positively with tensile forces acting on the fibers, indicating stress fibers as a tension sensor in ERK activation. Myosin II-dependent ERK activation is also observed on actomyosin bundles connecting E-cadherin clusters, thus suggesting that actomyosin bundles, in general, work as a platform for tension-dependent ERK activation.

Introduction

A growing body of research suggests that not only chemical cues such as growth factors and cytokines but also intracellular and extracellular mechanical environments have a significant impact on cellular behaviors including adhesion, migration, survival, proliferation and differentiation [1,2]. Adherent types of cells such as fibroblasts and endothelial cells adhere to extracellular matrix (ECM) substrates through the integrin-mediated adhesion structures called focal adhesions (FAs) [3]. Adhesion to ECM is necessary for survival and proliferation of normal but not transformed adherent cells ("anchorage-dependency" of cell growth) [4]. On the cytoplasmic side, FAs are connected to tips of the contractile actomyosin bundles called stress fibers (SFs). The actomyosin-generated contractile forces are transmitted to ECM through FAs, resulting in development of mechanical tension in the SF–FA–ECM complex [5]. A decrease in tension within the SF–FA–ECM complex caused by either actin cytoskeleton disruption, inhibition of actomyosin contractility or compliant ECM substrates results in inhibition of cell proliferation and affects lineage specification of stem cells [6,7]. This suggests an essential role of tension in regulating cell growth and differentiation.

Tension generated by the contractility of SFs and transmitted to FAs has been shown to regulate the formation and maintenance of these structures in a positive feedback fashion [5,8,9]. Since a variety of signaling molecules such as kinases, phosphatases and scaffold proteins accumulate at FAs and SFs [3,10], these structures have ideal properties to act as tension-regulated platforms for signal transduction [11,12]. On the one hand, various mechanotransduction events including phosphorylation of FAK, paxillin and p130Cas occur at FAs [13,14]. On the other hand, although forces exerted by SFs are critical for driving mechanotransduction events at FAs [15–18], the possible role of SFs per se as a signaling platform has not been extensively studied.

The extracellular signal-regulated kinase (ERK) subfamily of MAP kinases is involved in the regulation of diverse cellular functions including adhesion, migration, cell cycle progression, cytokinesis, proliferation, differentiation, senescence and cell death [19]. While localization of ERK to the actin cytoskeleton and FAs has been reported [20–25], its activation (phosphorylation at the threonine and tyrosine residues in the activation loop) is interestingly influenced by intracellular and extracellular mechanical cues. Rho–Rho kinase-mediated activation of actomyosin contractility is required for ERK activation [26,27]. Disruption of the actin cytoskeleton [28,29], inhibition of myosin II activity [30,31] or culturing cells on soft ECM substrates [32–34] diminishes activation of ERK. Additionally, mechanical stretching of ECM substrates on which cells adhere increases ERK activity [35,36]. All these results suggest the importance of tension along the SF–FA–ECM axis in ERK

1 Mechanobiology Institute, National University of Singapore, Singapore, Singapore
2 Department of Biomedical Engineering, National University of Singapore, Singapore, Singapore
3 Department of Mechanical Engineering, National University of Singapore, Singapore, Singapore
4 Institut Jacques Monod (IJM), CNRS UMR 7592, Université Paris Diderot, Paris, France
5 Mechanobiology Laboratory, Nagoya University Graduate School of Medicine, Nagoya, Japan
  *Corresponding author. Tel: +81 52 744 2051; Fax: +81 52 744 2057; E-mail: msokabe@med.nagoya-u.ac.jp
  †Present address: L'oreal Research and Innovation, Singapore, Singapore

activation. However, since the quantitative relationship between the tension magnitude and ERK activation has not been studied, the actual role of tension in ERK activation remains unclear. Furthermore, the mechanism by which the tension is transduced into ERK activation is unknown.

In this study, we examined the potential role of SFs as a platform for tension-dependent signaling events, with a particular focus on their role in ERK activation.

Results and Discussion

Immunofluorescence staining showed that activated ERK (phosphorylated ERK; pERK) localized to SFs in human foreskin fibroblasts (HFFs) (Fig 1A, Supplementary Fig S1A) and mouse NIH3T3 cells (Supplementary Fig S2). This was confirmed with two different antibodies both of which specifically recognized pERK in immunoblotting (Supplementary Fig S3). Distribution of pERK on SFs was exclusive to that of α-actinin, and pERK was not apparently localized at FAs (Supplementary Fig S4). ERK2 was preferentially phosphorylated in HFFs rather than ERK1, and shRNA-mediated depletion of ERK2 but not ERK1 expression significantly reduced pERK intensity on SFs (Supplementary Fig S5). Inhibition of myosin II activity with blebbistatin resulted in a drastic decrease in the amount of pERK on SFs; while there were residual SFs in blebbistatin-treated HFFs (Supplementary Fig S6) [17,18], the relative intensity of pERK against F-actin on SFs was significantly decreased upon the blebbistatin treatment (Fig 1A and B, Supplementary Fig S2). By contrast, the intensity ratio of total ERK against F-actin on SFs was not decreased by myosin II inhibition (Fig 1B and C). Similar results were obtained with confocal microscopy (Supplementary Fig S1B–D). These results indicate that ERK localizes on SFs regardless of myosin II activity, but it is phosphorylated or activated in a myosin II-dependent manner. Consistently, when cells were double-stained for pERK and total ERK, high ratio values of pERK/ERK on SFs were dissipated by the treatment with blebbistatin (Fig 1D). The mean value of pERK/ERK ratio in the entire cell region was decreased to about half ($51 \pm 15\%$) upon blebbistatin treatment (Fig 1D, bar graph), which was consistent with the result of immunoblotting analysis ($58 \pm 14\%$; Supplementary Fig S7A). This suggests that 40–50% of ERK phosphorylation is dependent on myosin II activity. While nuclear localization of pERK was also dependent on myosin II activity (Supplementary Fig S8), the relationship between ERK phosphorylation on SFs and its nuclear translocation needs to be revealed in future studies.

In order to examine the effect of tension within the SF–FA–ECM complex on ERK phosphorylation on SFs, myosin II-inhibited cells were subjected to external mechanical forces by uniaxially stretching fibronectin (FN)-coated elastic substrata. A sustained uniaxial stretch (50%, 5 min) caused a ~60% increase in phosphorylation of ERK in blebbistatin-treated cells (Supplementary Fig S7A). Stretching also resulted in reinforcement of SFs oriented along the stretch axis compared to those oriented perpendicular to the stretch axis or SFs in unstretched control cells (Fig 2A, Supplementary Fig S9, see also Supplementary Movie S1). A 5-min (Supplementary Fig S9) or 30-min (not shown) stretch did not induce apparent reorientation of SFs and cells in the presence of blebbistatin. The F-actin amount in individual SFs in their width direction was larger when SFs were

oriented at smaller angles against the stretch axis; SFs with the angles of 0–30° had the ~2.3-fold larger amount of F-actin compared with SFs with the angles of 60–90° (Fig 2B). Actin polymerization mediated by zyxin–VASP complexes and/or mDia1 [17,37,38], and/or self-remodeling of actomyosin meshwork into bundles [39] may be involved in the force-induced reinforcement of SFs. Intensity of pERK was higher on SFs parallel to the stretch axis compared to those perpendicular to the stretch axis or SFs in unstretched control cells (Fig 2A). When examined quantitatively, the intensity of pERK on SFs showed a negative correlation with the orientation of the SF (angle with respect to the stretch axis) (Fig 2C).

Uniaxial stretch-induced strain in SFs, whose tips are anchored to substrata through FAs, would vary with orientation of SFs with respect to the stretch axis. The strain (S) along the length of an SF can be expressed as a function of SF orientation, as

$$S = \sqrt{(1 + a/100)^2 \cos^2 \theta + \sin^2 \theta} - 1, \qquad (1)$$

where θ is the SF angle against the stretch axis and a is the percentage of stretch (see Supplementary Information for derivation). As shown above, SFs were reinforced by uniaxial stretching in a manner dependent on SF orientation (Fig 2B). By converting the SF angles in Fig 2B into SF strain using the equation [1], we obtained the relationship between the F-actin amount in individual SFs in their width direction and SF strain induced by 50% stretch (Supplementary Fig S10). Assuming that tensile elasticity of an SF (k) is proportional to the amount of F-actin (n) in the width direction of the SF, tensile force (F) developed in the SF upon stretching would also be proportional to the F-actin amount as $F = kS \propto nS$. Therefore, we can calculate relative tensile forces in SFs by using values of the F-actin amount and strain of individual SFs in Supplementary Fig S10 and obtained the tensile force–strain relationship of SFs as shown in Fig 2D. Relative tensile forces in SFs were increased quadratically, not linearly, with increasing strain (Fig 2D), which is consistent with previous results of force–strain measurements for isolated, single SFs in vitro [40] and suggests the strain-induced stiffening behavior of SFs. When SF angles in Fig 2C were converted into tensile forces developed in SFs by using the equation [1] and the regression equation in Fig 2D, we obtained a relationship between relative tensile forces in SFs and intensities of pERK on the SFs as shown in Fig 2E. There was a positive correlation between tensile forces and pERK intensities for individual SFs (Fig 2E). Similar correlation was obtained even for SFs within a single cell (Supplementary Fig S11). These results demonstrate that stretch-induced tension development in SFs causes ERK phosphorylation on SFs in myosin II-inhibited cells.

Stretching also increased phosphorylation of RSK, a major downstream effector of ERK [41], in blebbistatin-treated cells (Supplementary Fig S12). Stretch-induced phosphorylation of ERK and RSK was abolished when SFs were disrupted upon cytochalasin D treatment (Supplementary Fig S12), suggesting a critical role of SFs in stretch-induced activation of ERK and its downstream signal. In cells not treated with blebbistatin, stretching substrata did not increase ERK phosphorylation (Supplementary Fig S7B), implying that the endogenous level of myosin II-based tension is high enough for full phosphorylation of the tension-regulated population of ERK.
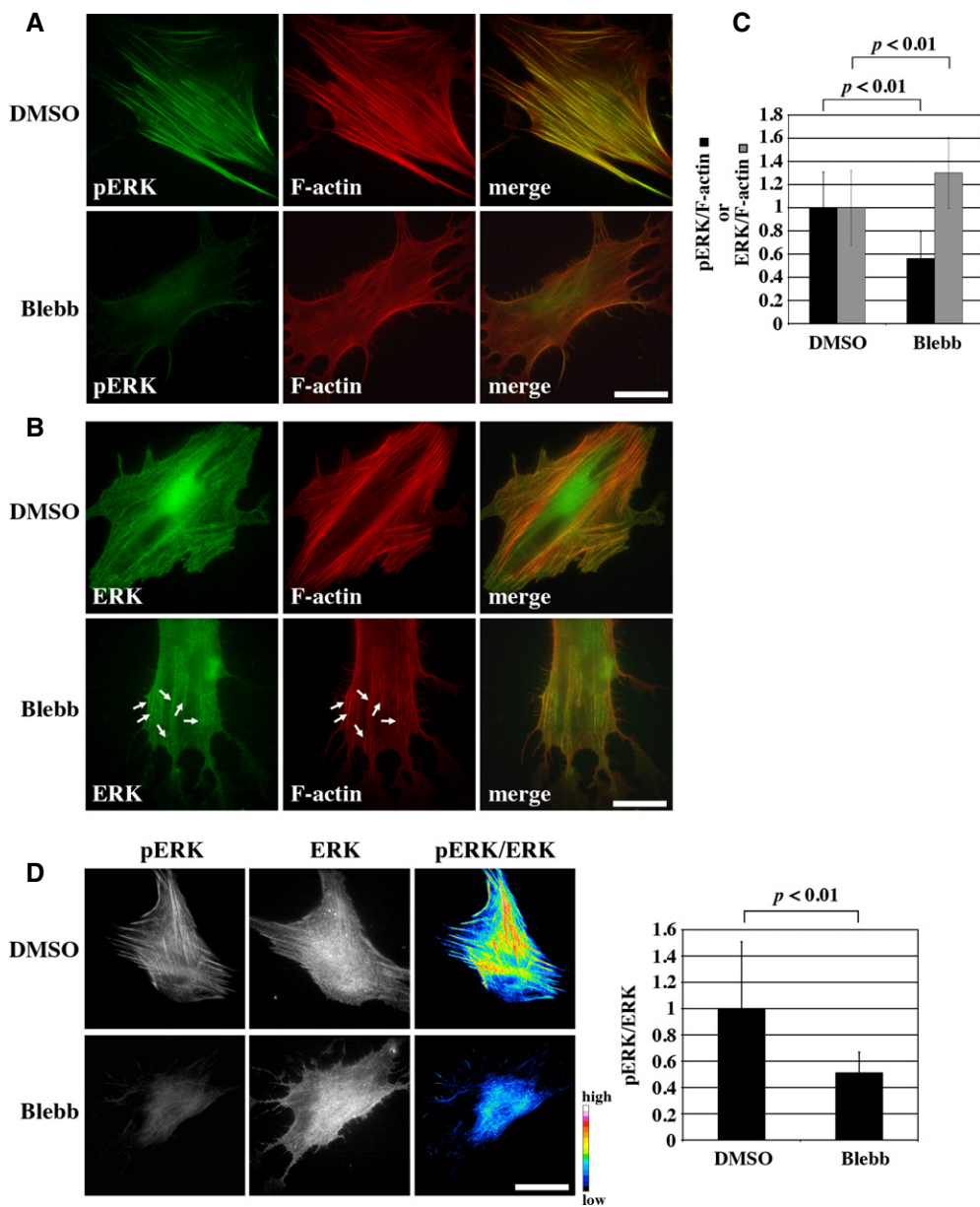
Figure 1. ERK is phosphorylated on SFs in a myosin II-dependent manner.

A, B   HFFs treated with either DMSO or 100 μM blebbistatin (Blebb) for 30 min were double-stained for F-actin and either pERK (A) or total ERK (B). Merged images are also shown. Arrows in (B) denote ERK localization on F-actin bundles in blebbistatin-treated cells. Scale bars, 40 μm.

C   Quantification results of intensity ratios of pERK (black bar) and ERK (gray bar) against F-actin on individual SFs in HFFs treated with either DMSO or 100 μM blebbistatin (Blebb). Sample values were normalized with respect to the mean values of control (DMSO) samples. *P*-values were calculated using Student's *t*-test. 118 SFs in 12 cells (pERK, DMSO), 103 SFs in 13 cells (pERK, Blebb), 150 SFs in 15 cells (ERK, DMSO) and 98 SFs in 12 cells (ERK, Blebb) were analyzed.

D   HFFs treated with either DMSO or 100 μM blebbistatin (Blebb) for 30 min were double-stained for pERK and total ERK. Ratio images of pERK against total ERK were calculated (pERK/ERK). The ratio values are shown in pseudo-color (arbitrary units). Scale bar, 40 μm. The bar graph shows mean values of the pERK/ERK ratio in individual cells. Sample values were normalized with respect to the mean value of control (DMSO) cells. *n* = 12 and 11 for DMSO and Blebb, respectively.

To further examine the tension–ERK phosphorylation relationship on SFs, we directly measured tensile forces within individual SFs using microforce sensor arrays (μFSA) [42,43]. Cells grown on μFSA with pillars whose tips were coated with FN were fixed and double-stained for pERK and F-actin (Fig 3A). Pillars to which tips of SFs were connected deflected inward along SFs (Fig 3A, see insets), showing transmission of contractile forces from SFs to pillars. The intensity of pERK was higher on SFs exerting larger forces (Fig 3B). Cells treated with blebbistatin showed a decrease in both force exertion by SFs and ERK phosphorylation on the SFs (Fig 3A and B). Thus, there was a clear positive correlation between tensile forces acting along SFs and ERK phosphorylation on SFs (Fig 3B). These results again support the notion that tension development in SFs facilitates phosphorylation of ERK on SFs.
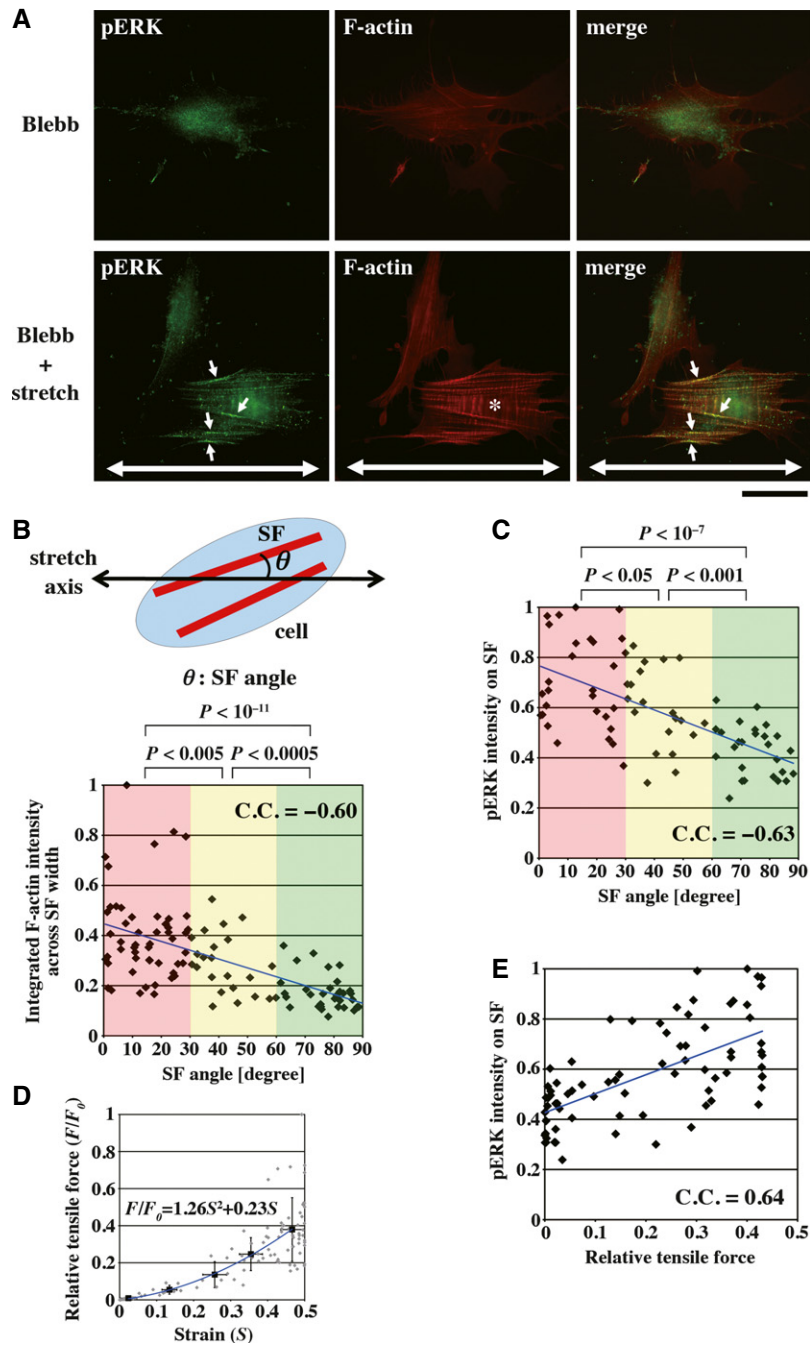
Figure 2. Mechanical stretch of myosin II-inhibited cells induces ERK phosphorylation on SFs in a manner dependent on tensile forces developed in SFs.

A   HFFs cultured on FN-coated elastic substrata were treated with 100 μM blebbistatin for 30 min, and then, the substrata were uniaxially stretched (50% for 5 min) in the presence of blebbistatin. Cells without (Blebb) or with stretching (Blebb + stretch) were double-stained for pERK and F-actin. Merged images are also shown. Double-headed arrows indicate the direction of stretching. In cells aligned along the stretch axis (*), high intensities of pERK on SFs were observed (arrows). Scale bar, 40 μm.

B   Top: Schematic representation of definition of the SF angle. Bottom: The integrated intensity of F-actin on each SF in its width direction was plotted against the SF angle. Intensities were normalized with respect to the maximum value. *P*-values were calculated using Student's *t*-test between groups in different ranges of SF angles ($0° \leq \theta < 30°$, $30° \leq \theta < 60°$ and $60° \leq \theta < 90°$). The blue line represents the linear fitting. C.C., correlation coefficient.

C   The averaged intensities of pERK along individual SFs were plotted against the SF angles. Intensities were normalized with respect to the maximum value.

D   Relative tensile forces and strain induced by 50% stretch were plotted for individual SFs (gray diamonds). Values of tensile forces were normalized with respect to the maximum value. Means ± SD in the windows of every 0.1 strain are also shown (black squares). The blue line represents the quadratic fitting of black squares.

E   For the same data set as that in (C), the averaged intensities of pERK along individual SFs were re-plotted against relative tensile forces in the SFs. Intensities were normalized with respect to the maximum value. The blue line represents the linear fitting.
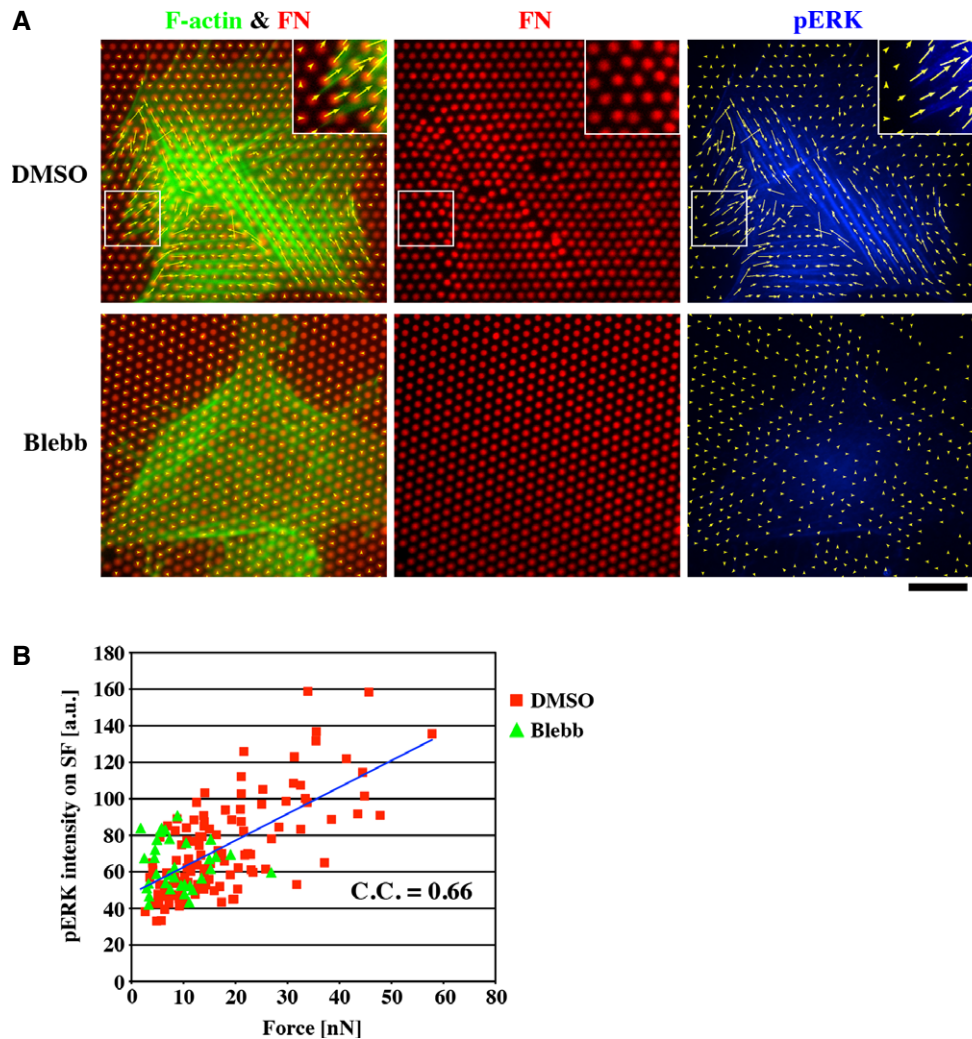
Figure 3. ERK phosphorylation on SFs depends on myosin II-generated contractile forces in SFs.

A HFFs cultured on arrays of pillars, whose tips were coated with ATTO 647-labeled FN, were treated with either DMSO or 100 μM blebbistatin (Blebb) for 30 min and then double-stained for F-actin and pERK. Forces exerted on pillars (yellow arrows) were calculated from positions of pillar tips as described in the Supplementary Information. Insets show magnified images of outlined regions. Scale bar (black), 20 μm, and force bar (yellow), 100 nN.

B The average intensity of pERK in each SF region within 5 μm from the SF tip was plotted against measured contractile force generated in the SF. The blue line represents the linear fitting. C.C., correlation coefficient.

Previous studies with laser cutting of SFs have shown that tension in SF–FA–ECM complexes plays a role in regulating cell shape and protein localization at SFs and FAs [15,44–46]. However, the actual magnitude of tension has not been measured in these studies. Here, we quantified tensile forces and ERK phosphorylation on individual SFs. Regardless of myosin II- or stretch-origin of force, phosphorylation of ERK on SFs was increased almost linearly with increasing tensile forces acting on SFs (Supplementary Figs S2E and S3B). This suggests that the tensile force is the "true" factor that induces ERK phosphorylation on SFs. Even in a single cell, SFs with larger tensile forces showed higher intensities of pERK (Fig 3A, Supplementary Fig S11), indicating that the tension-induced ERK phosphorylation is regulated at the individual SF level in a cell. Tension in SFs increases pERK in a synergistic way by increasing both the F-actin amount (Fig 2 and Supplementary Fig S6) and the pERK/F-actin ratio (Fig 1 and

Supplementary Fig S1) in each fiber. Thus, our results demonstrated that each SF per se works as a mechanotransduction platform which senses and transduces tension in the fiber into ERK activation.

Actomyosin bundles are formed not only between FAs (i.e., classical SFs) but also between cell–cell junctions [47,48]. We therefore extended our study to actomyosin bundles connecting cell–cell junctions and examined whether these actomyosin bundles also yield tension-dependent ERK phosphorylation. For this purpose, we used a recently developed assay system that allows the formation of suspended "epithelial bridges" [49]. In this context, a multicellular epithelial sheet was suspended over the ECM-devoid region, and cells in the bridge were held together by tensed actomyosin bundles interconnected through cell–cell junctions [49] (Supplementary Fig S13). Phosphorylated ERK was localized along interconnected actin bundles in the bridge of HaCaT keratinocytes (Fig 4A). It is
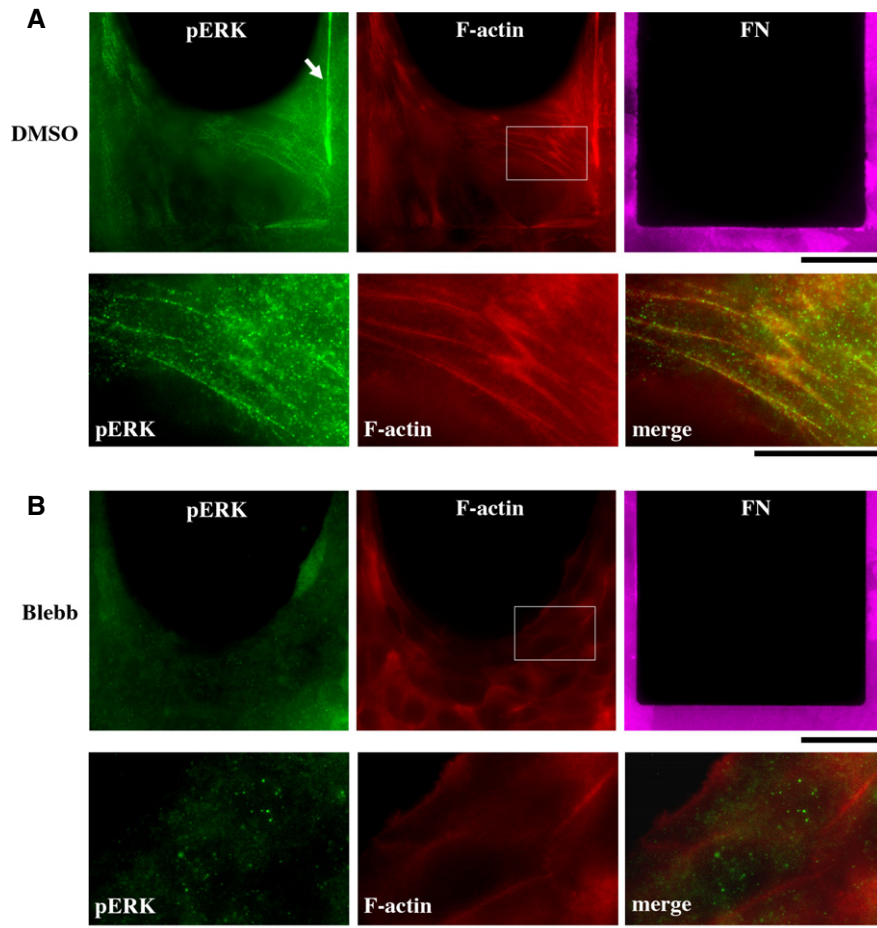
Figure 4. Myosin II-dependent ERK phosphorylation on actomyosin bundles in suspended epithelial bridges.

A, B   HaCaT cells on the fibronectin (FN) pattern formed epithelial bridges over FN-devoid, non-adhesive regions. The epithelial bridges were treated with either DMSO (A) or 100 μM blebbistatin (Blebb) (B) for 30 min and then double-stained for pERK and F-actin. The arrow indicates strong ERK phosphorylation on the actomyosin bundle along the edge of FN region. Lower panels: Magnified images of outlined regions in upper panels. Merged images are also shown. Scale bars, 40 μm for upper panels and 20 μm for lower panels.

noteworthy that while actin bundles in the suspended bridge were rich in pERK, F-actin accumulation at cell–cell boundaries on FN regions did not show any local increase in pERK (Supplementary Fig S14), indicating that accumulated F-actin is not sufficient to localize pERK. To test the effect of actomyosin-based tension on ERK phosphorylation in the epithelial bridge, the bridge was treated with blebbistatin. The tensed actin bundles were largely disassembled in the blebbistatin-treated bridge (Fig 4B). Instead, accumulations of F-actin at cell–cell junctions became obvious; however, pERK was not localized at these F-actin accumulations (Fig 4B). Thus, pERK localization on classical SFs as well as non-SF actomyosin bundles was dependent on myosin II activity. This implies that actomyosin bundles generally serve as a tension sensor and a platform for ERK activation.

The molecular mechanism of how tension in actomyosin bundles induces ERK phosphorylation on the bundles is unknown at present. ERK would localize to the actin cytoskeleton through direct binding with actin and/or binding via actin-binding proteins including calponins, α-actinin and IQGAP1 [23,50]. Of these actin-binding

proteins, IQGAP1 is of particular interest, because this protein is reportedly involved in both ERK localization to the actin cytoskeleton and phosphorylation of actin-associated ERK [23]. FAK and Src signaling at FAs has been suggested to be involved in ERK phosphorylation in response to mechanical stimuli [34,36,51,52]. Consistently, inhibition of Src or FAK largely reduced ERK phosphorylation on SFs (Supplementary Fig S15). In epithelial bridges, strong ERK phosphorylation was observed on actomyosin bundles along edges of FN regions (arrow in Fig 4A), which may reflect that integrin-mediated Src and FAK signaling evokes ERK phosphorylation on the bundles. In addition, serum-induced signaling was required for elevation of ERK phosphorylation upon substratum stretching, even though ERK was localized to the actin cytoskeleton in serum-starved cells (Supplementary Fig S16). Thus, serum- and/or integrin-mediated signaling and cytoskeletal tension are both involved in ERK phosphorylation. Actomyosin bundles are likely to serve as a platform for integrating these chemical and mechanical signals. Future studies are needed to unveil molecular details underlying tension-dependent phosphorylation of ERK on

actomyosin bundles. They include revealing which molecule senses tension in actomyosin bundles and how the sensed tension is transduced into the signal that facilitates ERK phosphorylation on the bundles.

Materials and Methods

Cell culture

Human foreskin fibroblasts (HFFs), NIH3T3 and HaCaT (Cell Lines Service, Eppelheim, Germany) cells were maintained in high-glucose Dulbecco's modified Eagle's medium (Life Technologies, Carlsbad, CA) supplemented with 10% fetal bovine serum (Life Technologies). For experiments, HFFs and NIH3T3 cells were grown for ~15 h on glass coverslips, elastic silicone [polydimethyl siloxane (PDMS)] chambers (Strex, Osaka, Japan) precoated with 50 μg/ml FN (Sigma Chemical, St. Louis, MO) or μFSA substrates with pillars whose tips were coated with ATTO 647 (Sigma Chemical)-conjugated FN. Epithelial bridges of HaCaT cells were prepared as we reported recently [49].

Acknowledgements

Author contributions

HH, BL and MS designed the research. HH performed the experiments. HH and MG analyzed the data. MG and SRKV prepared microfabricated substrates. HH, CTL, BL and MS wrote the manuscript.

Conflict of interest

The authors declare that they have no conflict of interest.

References

1. Discher DE, Janmey P, Wang YL (2005) Tissue cells feel and respond to the stiffness of their substrate. *Science* 310: 1139–1143

2. Parsons JT, Horwitz AR, Schwartz MA (2010) Cell adhesion: integrating cytoskeletal dynamics and cellular tension. *Nat Rev Mol Cell Biol* 11: 633–643

3. Geiger B, Spatz JP, Bershadsky AD (2009) Environmental sensing through focal adhesions. *Nat Rev Mol Cell Biol* 10: 21–33

4. Chiarugi P, Giannoni E (2008) Anoikis: a necessary death program for anchorage-dependent cells. *Biochem Pharmacol* 76: 1352–1364

5. Chrzanowska-Wodnicka M, Burridge K (1996) Rho-stimulated contractility drives the formation of stress fibers and focal adhesions. *J Cell Biol* 133: 1403–1415

6. Engler AJ, Sen S, Sweeney HL, Discher DE (2006) Matrix elasticity directs stem cell lineage specification. *Cell* 126: 677–689

7. Assoian RK, Klein EA (2008) Growth control by intracellular tension and extracellular stiffness. *Trends Cell Biol* 18: 347–352

8. Ladoux B, Nicolas A (2012) Physically based principles of cell adhesion mechanosensitivity in tissues. *Rep Prog Phys* 75: 116601

9. Balaban NQ, Schwarz US, Riveline D, Goichberg P, Tzur G, Sabanay I, Mahalu D, Safran S, Bershadsky A, Addadi L *et al* (2001) Force and focal adhesion assembly: a close relationship studied using elastic micro-patterned substrates. *Nat Cell Biol* 3: 466–472

10. Tojkander S, Gateva G, Lappalainen P (2012) Actin stress fibers – assembly, dynamics and biological roles. *J Cell Sci* 125: 1855–1864

11. Nicolas A, Geiger B, Safran SA (2004) Cell mechanosensitivity controls the anisotropy of focal adhesions. *Proc Natl Acad Sci U S A* 101: 12520–12525

12. Plotnikov SV, Pasapera AM, Sabass B, Waterman CM (2012) Force fluctuations within focal adhesions mediate ECM-rigidity sensing to guide directed cell migration. *Cell* 151: 1513–1527

13. Sawada Y, Tamada M, Dubin-Thaler BJ, Cherniavskaya O, Sakai R, Tanaka S, Sheetz MP (2006) Force sensing by mechanical extension of the Src family kinase substrate p130Cas. *Cell* 127: 1015–1026

14. Pasapera AM, Schneider IC, Rericha E, Schlaepfer DD, Waterman CM (2010) Myosin II activity regulates vinculin recruitment to focal adhesions through FAK-mediated paxillin phosphorylation. *J Cell Biol* 188: 877–890

15. Lele TP, Pendse J, Kumar S, Salanga M, Karavitis J, Ingber DE (2006) Mechanical forces alter zyxin unbinding kinetics within focal adhesions of living cells. *J Cell Physiol* 207: 187–194

16. Hayakawa K, Tatsumi H, Sokabe M (2008) Actin stress fibers transmit and focus force to activate mechanosensitive channels. *J Cell Sci* 121: 496–503

17. Hirata H, Tatsumi H, Sokabe M (2008) Mechanical forces facilitate actin polymerization at focal adhesions in a zyxin-dependent manner. *J Cell Sci* 121: 2795–2804

18. Hirata H, Tatsumi H, Lim CT, Sokabe M (2014) Force-dependent vinculin binding to talin in live cells: a crucial step in anchoring the actin cytoskeleton to focal adhesions. *Am J Physiol Cell Physiol* 306: C607–C620

19. Ramos JW (2008) The regulation of extracellular signal-regulated kinase (ERK) in mammalian cells. *Int J Biochem Cell Biol* 40: 2707–2719

20. Fincham VJ, James M, Frame MC, Winder SJ (2000) Active ERK/MAP kinase is targeted to newly forming cell-matrix adhesions by integrin engagement and v-Src. *EMBO J* 19: 2911–2923

21. Zuckerbraun BS, Shapiro RA, Billiar TR, Tzeng E (2003) RhoA influences the nuclear localization of extracellular signal-regulated kinases to modulate p21$^{Waf/Cip1}$ expression. *Circulation* 108: 876–881

22. Pritchard CA, Hayes L, Wojnowski L, Zimmer A, Marais RM, Norman JC (2004) B-Raf acts via the ROCKII/LIMK/cofilin pathway to maintain actin stress fibers in fibroblasts. *Mol Cell Biol* 24: 5937–5952

23. Vetterkind S, Poythress RH, Lin QQ, Morgan KG (2013) Hierarchical scaffolding of an ERK1/2 activation pathway. *Cell Commun Signal* 11: 65

24. Appel S, Allen PG, Vetterkind S, Jin JP, Morgan KG (2010) h3/Acidic calponin: an actin-binding protein that controls extracellular signal-regulated kinase 1/2 activity in nonmuscle cells. *Mol Biol Cell* 21: 1409–1422

25. Vetterkind S, Saphirstein RJ, Morgan KG (2012) Stimulus-specific activation and actin dependency of distinct, spatially separated ERK1/2 fractions in A7r5 smooth muscle cells. *PLoS ONE* 7: e30409

26. Renshaw MW, Toksoz D, Schwartz MA (1996) Involvement of the small GTPase Rho in integrin-mediated activation of mitogen-activated protein kinase. *J Biol Chem* 271: 21691–21694

27. Welsh CF, Roovers K, Villanueva J, Liu Y, Schwartz MA, Assoian RK (2001) Timing of cyclin D1 expression within G1 phase is controlled by Rho. *Nat Cell Biol* 3: 950–957

28. Tsakiridis T, Bergman A, Somwar R, Taha C, Aktories K, Cruz TF, Klip A, Downey GP (1998) Actin filaments facilitate insulin activation of the Src and collagen homologous/mitogen-activated protein kinase pathway leading to DNA synthesis and *c-fos* expression. *J Biol Chem* 273: 28322–28331

29. Numaguchi K, Eguchi S, Yamakawa T, Motley ED, Inagaki T (1999) Mechanotransduction of rat aortic vascular smooth muscle cells requires RhoA and intact actin filaments. *Circ Res* 85: 5–11

30. Helfman DM, Pawlak G (2005) Myosin light chain kinase and acto-myosin contractility modulate activation of the ERK cascade down-stream on oncogenic Ras. *J Cell Biochem* 95: 1069–1080

31. Kim JH, Wang A, Conti MA, Adelstein RS (2012) Nonmuscle myosin II is required for internalization of the epidermal growth factor receptor and modulation of downstream signaling. *J Biol Chem* 287: 27345–27358

32. Rosenfeldt H, Grinnell F (2000) Fibroblast quiescence and the disruption of ERK signaling in mechanically unloaded collagen matrices. *J Biol Chem* 275: 3088–3092

33. Paszek MJ, Zahir N, Johnson KR, Lakins JN, Rozenberg GI, Gefen A, Reinhart-King CA, Margulies SS, Dembo M, Boettiger D *et al* (2005) Tensional homeostasis and the malignant phenotype. *Cancer Cell* 8: 241–254

34. Shih YRV, Tseng KF, Lai HY, Lin CH, Lee OK (2011) Matrix stiffness regu-lation of integrin-mediated mechanotransduction during osteogenic differentiation of human mesenchymal stem cells. *J Bone Miner Res* 26: 730–738

35. Sawada Y, Nakamura K, Doi K, Takeda K, Tobiume K, Saitoh M, Morita K, Komuro I, De Vos K, Sheetz M *et al* (2001) Rap1 is involved in cell stretching modulation of p38 but not ERK or JNK MAP kinase. *J Cell Sci* 114: 1221–1227

36. Li Y, Gallant C, Malek S, Morgan KG (2007) Focal adhesion signaling is required for myometrial ERK activation and contractile phenotype switch before labor. *J Cell Biochem* 100: 129–140

37. Yoshigi M, Hoffman LM, Jensen CC, Yost J, Beckerle MC (2005) Mechani-cal force mobilizes zyxin from focal adhesions to actin filaments and regulates cytoskeletal reinforcement. *J Cell Biol* 171: 209–215

38. Rao MV, Chu PH, Hahn KM, Zaidel-Bar R (2013) An optogenetic tool for the activation of endogenous diaphanous-related formins induces thick-ening of stress fibers without an increase in contractility. *Cytoskeleton* 70: 394–407

39. Hirata H, Tatsumi H, Sokabe M (2007) Dynamics of actin filaments during tension-dependent formation of actin bundles. *Biochim Biophys Acta* 1770: 1115–1127

40. Deguchi S, Ohashi T, Sato M (2006) Tensile properties of single stress fibers isolated from cultured vascular smooth muscle cells. *J Biomech* 39: 2603–2610

41. Anjum R, Blenis J (2008) The RSK family of kinases: emerging roles in cellular signalling. *Nat Rev Mol Cell Biol* 9: 747–758

42. Tan JL, Tien J, Pirone DM, Gray DS, Bhadriraju K, Chen CS (2003) Cells lying on a bed of microneedles: an approach to isolate mechanical force. *Proc Natl Acad Sci U S A* 100: 1484–1489

43. Trichet L, Le Digabel J, Hawkins RJ, Vedula SRK, Gupta M, Ribrault C, Hersen P, Voituriez R, Ladoux B (2012) Evidence of a large-scale mechanosensing mechanism for cellular adaptation to substrate stiff-ness. *Proc Natl Acad Sci U S A* 109: 6933–6938

44. Kumar S, Maxwell IZ, Heisterkamp A, Polte TR, Lele TP, Salanga M, Mazur E, Ingber DE (2006) Viscoelastic retraction of single living stress fibers and its impact on cell shape, cytoskeletal organiza-tion, and extracellular matrix mechanics. *Biophys J* 90: 3762–3773

45. Colombelli J, Besser A, Kress H, Reynaud EG, Girard P, Caussinus E, Haselmann U, Small JV, Schwarz US, Stelzer EHK (2009) Mechanosensing in actin stress fibers revealed by a close correlation between force and protein localization. *J Cell Sci* 122: 1665–1679

46. Tanner K, Boudreau A, Bissell MJ, Kumar S (2010) Dissecting regional variations in stress fiber mechanics in living cells with laser nanosur-gery. *Biophys J* 99: 2775–2783

47. Hinz B, Pittet P, Smith-Clerc J, Chaponnier C, Meister JJ (2004) Myofibro-blast development is characterized by specific cell-cell adherens junc-tions. *Mol Biol Cell* 15: 4310–4320

48. Millán J, Cain RJ, Reglero-Real N, Bigarella C, Marcos-Ramiro B, Fernández-Martín L, Correas I, Ridley AJ (2010) Adherens junctions connect stress fibers between adjacent endothelial cells. *BMC Biol* 8: 11

49. Vedula SRK, Hirata H, Nai MH, Brugués A, Toyama Y, Trepat X, Lim CT, Ladoux B (2014) Epithelial bridges maintain tissue integrity during collective cell migration. *Nat Mater* 13: 87–96

50. Leinweber BD, Leavis PC, Grabarek Z, Wang CLA, Morgan KG (1999) Extracellular regulated kinase (ERK) interaction with actin and the calponin homology (CH) domain of actin-binding proteins. *Biochem J* 344: 117–123

51. Li Y, Reznichenko M, Tribe RM, Hess PE, Taggart M, Kim HR, DeGnore JP, Gangopadhyay S, Morgan KG (2009) Stretch activates human myometrium via ERK, caldesmon and focal adhesion signaling. *PLoS ONE* 4: e7489

52. Hong SY, Jeon YM, Lee HJ, Kim JG, Baek JA, Lee JC (2010) Activation of RhoA and FAK induces ERK-mediated osteopontin expression in mechanical force-subjected periodontal ligament fibroblasts. *Mol Cell Biochem* 335: 263–272